



CDF/PHYS/TOP/PUB/11232

# Measurement of the Top Quark Polarization using Dilepton Channel in $t\bar{t}$ Production

The CDF Collaboration  
(Dated: February 28, 2018)

## Abstract

We present a measurement of the top quark polarization in the  $t\bar{t}$  pair production in  $p\bar{p}$  collisions at the Fermilab Tevatron collider at  $\sqrt{s}=1.96$  TeV. The final state events containing two leptons (electron or muon) with high transverse momentum, two jets and large transverse missing energy are analyzed using the full Run II data corresponding to  $9.1 \text{ fb}^{-1}$ . The top quark polarization are measured using the two dimensional angular distribution of leptons in the transverse base, where the reference axes are normal to the  $t\bar{t}$  production plane, and in the helicity base. The measurement is performed assuming that the polarization is generated by either a CP-conserving (CPC) or a CP-violating (CPV) production amplitude. The polarization is found to be negligible in both frames, as predicted by the Standard Model (SM).

The CDF and D0 experiments at the Fermilab Tevatron have measured the asymmetry of  $t\bar{t}$  pairs by measuring their rapidity distributions or the angular distributions of their decay leptons. The inclusive and differential asymmetries are consistent with the Standard Model (SM) predictions [1]. The polarization of  $t\bar{t}$  pairs as well as asymmetry is also important properties. The SM predicts nearly zero top quark polarization in top-antitop ( $t\bar{t}$ ) production from unpolarized hadron collisions, due to the parity-conserving nature of QCD [2, 3, 4], and the top quark polarization practically can be neglected even with the electroweak corrections [5]. On the other hand, some physics beyond the Standard Model (BSM), such as interaction amplitudes involving axi-gluons, might generate appreciable polarization by interfering with SM amplitudes, without spoiling the agreement of the production cross section with the SM prediction [5, 6].

As the life time of top quark is shorter than the time scale for hadronization, the spin state information of top quark remains in the angular distributions of its decay products. So top quark polarization can be measured from the angular distribution of its decay products with respect to a given quantization axis. In this analysis, the directions of the leptons of the  $t\bar{t}$  dilepton decay channel are used to measure top quark polarization. The double differential angular distribution of two leptons in the top (antitop) quark rest frame is given by

$$\frac{1}{\sigma} \frac{d^2\sigma}{d\cos\theta_+ d\cos\theta_-} = \frac{1}{4}(1 + \alpha_+ P_+ \cos\theta_+ + \alpha_- P_- \cos\theta_- - C \cos\theta_+ \cos\theta_-), \quad (1)$$

where  $\theta_{+(-)}$  is the opening angle between the positively (negatively) charged lepton with respect to the quantization axis in the top (antitop) quark rest frame,  $C$  is the  $t\bar{t}$  spin correlation coefficient,  $P_{+(-)}$  is the degree of polarization of the top (antitop) quark along the chosen quantization axis, and  $\alpha_{+(-)}$  is the spin-analyzing power of the positively (negatively) charged lepton, which is a measure of the sensitivity of the daughter particle to the spin state of the parent [2, 5]. At the leading order, charged leptons and down-type quarks from  $W$  boson decays are predicted to have the largest sensitivity to the spin state of the top quark with a spin-analyzing power of  $\alpha = 1$  [7], while for the b quark  $\alpha = -0.4$ .

In this analysis, the full data collected by the CDF detector during Run II corresponding to an integrated luminosity of  $9.1 \text{ fb}^{-1}$  is analyzed, and dilepton events ( $ee$ ,  $\mu\mu$ , and  $e\mu$ ) are selected. The event selection criteria used are same as in the previous CDF measurements of  $t\bar{t}$  production cross section and  $A_{FB}$  asymmetry in the dilepton channel [8, 9]. The detailed descriptions of data set, the Monte Carlo signal sample, the background, and the dilepton selection rules can be found in in Ref. [9]. The dilepton sample selection cuts are briefly summarized in the following.

- Opositely charged lepton pairs
  - electron  $E_T > 20 \text{ GeV}$
  - muon  $p_T > 20 \text{ GeV}/c$
  - $M_{l+l-} > 10 \text{ GeV}/c^2$
- At least two jets
  - $E_T > 15 \text{ GeV}$
  - $|\eta_{det}| < 2.5$
- $\cancel{E}_T$ 
  - $\cancel{E}_T > 25 \text{ GeV}$  if the angle between  $\vec{\cancel{E}}_T$  and any of lepton or jet azimuthal direction is grater than  $20^\circ$
  - $\cancel{E}_T > 50 \text{ GeV}$  else

- $H_T > 200$  GeV
- $Z$  veto for  $ee$  and  $\mu\mu$ 
  - Events are rejected if
    - \*  $76 < M_{l+l-} < 106$  GeV/ $c^2$
    - \*  $\frac{\cancel{E}_T}{\sqrt{\sum E_T}} > 4$  GeV $^{1/2}$

After applying the dilepton selection cuts, the number of observed candidates and the SM expectation of signal and backgrounds are shown to be in good agreements (see Table 1). These candidate events are then kinematically reconstructed by constraining leptons, jets, and neutrinos to form  $W$  mass, top mass,  $\cancel{E}_x$ , and  $\cancel{E}_y$  while scanning over neutrino momenta.

The methods for estimating signal and background follow Ref. [9]. The  $t\bar{t}$  signal MC sample is generated with the POWHEG NLO MC generator [10], which accounts for the SM strength spin correlation and spin polarization, followed by PYTHIA [11] for showering partons and the detailed CDFII detector simulation [12]. The backgrounds include events from the Drell-Yan production ( $Z/\gamma^*$ +jets),  $W$  production with jets ( $W$ +fake lepton), diboson production ( $WW$ ,  $WZ$ ,  $ZZ$ , and  $W\gamma$ ), and the  $t\bar{t}$  decaying to non-dilepton final states. The signal and backgrounds are listed in Table 1 which is taken from Ref. [9].

CDF Run II Prelim (9.1 fb $^{-1}$ )	
Source	Number of Events
$WW$	$21.1 \pm 4.2$
$WZ$	$5.8 \pm 1.0$
$ZZ$	$3.7 \pm 0.5$
$W\gamma$	$0.7 \pm 0.8$
DY $\rightarrow\tau\tau$	$17.0 \pm 2.8$
DY $\rightarrow ee/\mu\mu$	$33.5 \pm 3.9$
$W$ +fake lepton	$63.8 \pm 17.1$
$t\bar{t}$ non-dilepton	$14.7 \pm 0.8$
Total background	$160.3 \pm 21.2$
$t\bar{t}$ ( $\sigma = 7.4$ pb)	$408.2 \pm 19.4$
Total SM expectation	$568.5 \pm 40.3$
Observed ( $\mathcal{L} = 9.1$ fb $^{-1}$ )	569

Table 1: Table of expected and observed numbers of background and signal events after dilepton selection taken from Ref. [9]. The fake lepton is a jet misidentified as a lepton.

In this analysis, the spin polarization of top quark is measured in the helicity and transverse bases. In the helicity basis, the momentum directions of the top and antitop quarks in the  $t\bar{t}$  center-of-mass frame are defined as the quantization axes. In the transverse basis, the polarization of the top and antitop quarks perpendicular to the production plane is measured. The quantization axis of the top quark in the transverse basis is defined as the cross product of the proton momentum direction and the top quark momentum direction [13, 14], i.e.,

$$\hat{n}_p = \frac{\hat{p}_p \times \hat{k}}{|\hat{p}_p \times \hat{k}|}, \quad (2)$$

where  $\hat{p}_p$  is the unit vector of proton direction in the lab frame and  $\hat{k}$  is the unit vector of the top quark direction in the  $t\bar{t}$  rest frame. Table 2 shows the quantization axes for top ( $\hat{a}$ ) and antitop

Axis	Helicity	Transverse
$\hat{a}$	$\hat{k}$	$\frac{y_p}{ y_p } \hat{n}_p$
$\hat{b}$	$-\hat{k}$	$-\frac{y_p}{ y_p } \hat{n}_p$

Table 2: The quantization axes in the helicity and transverse bases. The axes in the transverse basis is defined as in Ref. [14].  $\hat{a}$  and  $\hat{b}$  are quantization axes for top and antitop quarks, respectively, as shown in Fig. 1.  $\hat{n}_p$  is defined in Eq. 2 and  $\hat{k}$  is the unit vector of the top quark direction in the  $t\bar{t}$  rest frame.

Basis	Spin Corr.		$\alpha P$ Physical Region	
	Theory	POWHEG	CPC	CPV
Helicity	-0.370	$-0.374 \pm 0.003$	$[-0.685, 0.685]$	$[-0.315, 0.315]$
Transverse	-	$0.168 \pm 0.003$	$[-0.416, 0.416]$	$[-0.584, 0.584]$

Table 3: The spin correlation coefficient from theory and physical regions of  $\alpha P$  in the beamline, helicity, and transverse bases for CPC and CPV.

( $\hat{b}$ ) in the helicity and transverse bases (see Fig. 1). To account for the Bose-symmetry of the  $gg$  initial state the signs of  $y_p = \hat{n}_p \cdot \hat{k}$  is required for the transverse basis quantization axes [15].

To make a signal ( $\cos \theta_+, \cos \theta_-$ ) template with a specific degree of polarization  $\alpha_{\pm} P_{\pm}$  each signal event is weighted by

$$f(\cos \theta_+, \cos \theta_-; \alpha_{\pm} P_{\pm}) = \frac{1 + \alpha_+ P_+ \cos \theta_+^p + \alpha_- P_- \cos \theta_-^p - C_{SM} \cos \theta_+^p \cos \theta_-^p}{1 - C_{temp} \cos \theta_+^p \cos \theta_-^p}, \quad (3)$$

where  $\theta_{+(-)}^p$  is the angle between the positively (negatively) charged lepton momentum and the respective quantization axis in the  $t(\bar{t})$ -quark rest frame calculated at the parton level and  $C_{SM}$  and  $C_{temp}$  are the spin correlation coefficients of the SM and templates in the given reference frame. The ( $\cos \theta_+, \cos \theta_-$ ) template is then constructed with weighted events. Figures 2 and 3 show the reconstructed ( $\cos \theta_+, \cos \theta_-$ ) distributions with  $\alpha P = 0$  and  $\pm 0.3$  in the helicity and transverse bases, respectively. The weighted signal templates in the regions are produced and compared with data to measure the polarization. In this analysis, two extreme CP assumptions are considered, the CP conserved(CPC)case where  $\alpha P^{CPC} = \alpha_+ P_+ = \alpha_- P_-$  and the CP maximally violated (CPV) case where  $\alpha P^{CPV} = \alpha_+ P_+ = -\alpha_- P_-$ . The physically allowed regions of  $\alpha P$  are listed on Table 3 for both of CPC and CPV.

The angular distribution from data is compared with the weighted signal template plus backgrounds and fitted to extract the best polarization values. The ( $\cos \theta_+, \cos \theta_-$ ) distribution of data can be compared with the those of the background and signal templates of various degree of polarization. The angular distributions of two leptons for all backgrounds are shown in the helicity and transverse bases in Figure. 4 and 5. Figure 6 and 7 compare data to the sum of weighted signal and total background in two dimensional distributions. The one dimensional distributions projected into  $\cos \theta_+$  and  $\cos \theta_-$  are compared in Figure. 8 and 9.

The  $\alpha P$  is extracted by using a likelihood fitting method. The likelihood is constructed

adopting the ‘‘pull approach’’ framework given in Ref. [16] as

$$\begin{aligned} \mathcal{L}(\alpha P) &= \left[ \frac{1}{\sqrt{2\pi}\sigma_s} \exp\left(-\frac{\delta_s^2}{2\sigma_s^2}\right) \right] \left[ \frac{1}{\sqrt{2\pi}\sigma_b} \exp\left(-\frac{\delta_b^2}{2\sigma_b^2}\right) \right] \\ &\times \left[ \prod_{i=bin} \frac{e^{-\lambda_i} \lambda_i^{n_i}}{n_i!} \frac{1}{\sqrt{2\pi}\sigma_{\xi_i}} \exp\left(-\frac{\xi_i^2}{2\sigma_{\xi_i}^2}\right) \right], \end{aligned} \quad (4)$$

where  $n_i$  and  $\lambda_i$  are the numbers of observed and expected events, respectively, in the  $i$ th bin,  $\delta_{s(b)}$  is the event ‘‘pull’’ parameter with respect to the total number of signal (background) events to be determined by fitting,  $\sigma_{s(b)}$  is the uncertainty of the number of signal (total background) events shown in Table 1, and  $\xi_i$  and  $\sigma_{\xi_i}$  are the pull parameter and the uncertainty coming from the statistical uncertainty of the background templates for the  $i$ th bin, respectively. The number of events in the  $i$ th bin determined by fitting is

$$\lambda_i = (\nu_s + \delta_s) \rho_{s_i}^{\alpha P} + (\nu_b + \delta_b) \left( \rho_{b_i} + \frac{\xi_i}{\nu_b} \right), \quad (5)$$

where  $\nu_{s(b)}$  are the expected number of signal (total background) shown in Table 1,  $\rho_{s_i}^{\alpha P}$  and  $\rho_{b_i}$  are the normalized event densities of signal with the degree of polarization of  $\alpha P$  and of background, respectively, in the  $i$ th bin. The statistical uncertainty of the background template is calculated as

$$(\sigma_{\xi_i})^2 = \sum_{j=bg} \left( c_j \sqrt{N_i^j} \right)^2, \quad (6)$$

where  $c_j$  is the normalization factor to the expected for the  $j$ th background and  $N_i^j$  is the number of events before the normalization in the  $i$ th bin of the  $j$ th background.

The first two terms in Eq. 4 constrain the measured total numbers of signal and background events to their expected values within uncertainties. The third term is the Poisson probability with the background constrained within the template statistical uncertainty in each bin. By introducing a pull  $\xi_i$  for each bin of the total background template, the uncertainty on the background shape coming from the statistical fluctuations in the total background template is accounted for as a penalty to the likelihood. The negative log likelihood,  $-\ln \mathcal{L}$ , is minimized by varying  $\delta_s$ ,  $\delta_b$ , and  $\xi_i$  to get the minimum  $-\ln \mathcal{L}$  value for the signal template with a given  $\alpha P$  and  $\rho_{s_i}^{\alpha P}$ .

To extract the best  $\alpha P$ , data are fitted with several  $\alpha P$  values and the obtained minimum  $-\ln \mathcal{L}$  are interpolated to get a smooth function. The likelihood fittings are performed for both of helicity basis (Fig. 10 (a) and (b)) and transverse basis (Fig. 10 (c) and (d)), for CPC and CPV. The best values of  $\alpha P$  are summarized in Table 4. Results are consistent with the SM expectations. The uncertainties are the sum of the statistical uncertainty of the data and the background shape uncertainty coming from the background template statistical uncertainty.

The likelihood in Eq. 4 has pulls for the numbers of signal and background expectations and the expected numbers in each bin of the total background template, each constrained by a Gaussian function to its uncertainty. Therefore, the uncertainties listed in Table 4 are not purely statistical in nature and the statistical uncertainty must be calculated by removing the pulls. The correct statistical uncertainty is obtained by removing all pulls, i.e., fixing all pulls to the expected mean values, from the likelihood in Eq. 4. The results are shown in Table 5.

Most systematic uncertainties are estimated by using MC samples affected by the systematics being considered. Those are the parton distribution functions (PDF), initial and final state radiation (ISR/FSR), jet energy scale (JES), renormalization scale ( $\mu$  scale), top quark mass, MC generator, color reconnection, and parton showering. Pseudo-data ( $\cos \theta_+$ ,  $\cos \theta_-$ ) distributions

CDF Run II Prelim (9.1 fb <sup>-1</sup> )		
$\alpha P$		
Helicity	CPC	$-0.130^{+0.117}_{-0.112}$
	CPV	$-0.046^{+0.126}_{-0.125}$
Transverse	CPC	$-0.077^{+0.182}_{-0.181}$
	CPV	$-0.111^{+0.149}_{-0.148}$

Table 4: Measured polarization from data in the helicity and transverse bases for CPC and CPV. The uncertainties are from the fit only, therefore, they include the statistical uncertainties along with the background template statistical uncertainties and expected signal and background yield uncertainties.

CDF Run II Prelim (9.1 fb <sup>-1</sup> )				
	Helicity		Transverse	
	CPC	CPV	CPC	CPV
Statistical Uncertainty	$^{+0.114}_{-0.109}$	$\pm 0.123$	$\pm 0.177$	$^{+0.146}_{-0.145}$

Table 5: The statistical uncertainties of  $\alpha P$  fit results in Table 4. The uncertainties are obtained by removing pulls in the likelihood in Eq. 4.

are generated using these MC samples and are weighted to the desired  $\alpha P$  values. The background shape uncertainty is the sum of the uncertainty from the background template fluctuation and the uncertainty in the contribution of each background.

The full data of 9.1 fb<sup>-1</sup> collected at CDF detector are analyzed and the results are

$$\alpha P_{\text{helicity}}^{\text{CPC}} = -0.130^{+0.114}_{-0.109} \text{ (stat.)} \pm 0.111 \text{ (syst.)} \quad (7)$$

$$\alpha P_{\text{helicity}}^{\text{CPV}} = -0.046 \pm 0.123 \text{ (stat.)} \pm 0.040 \text{ (syst.)} \quad (8)$$

$$\alpha P_{\text{transverse}}^{\text{CPC}} = -0.077 \pm 0.177 \text{ (stat.)} \pm 0.098 \text{ (syst.)} \quad (9)$$

$$\alpha P_{\text{transverse}}^{\text{CPV}} = -0.111^{+0.146}_{-0.145} \text{ (stat.)}^{+0.055}_{-0.056} \text{ (syst.)} \quad (10)$$

The measured polarizations are consistent with the SM predictions. Figure 11 is a summary of measurement of top quark polarization in the dilepton channel at the Tevatron.

## References

- [1] T. A. Aaltonen *et al.* [CDF and D0 Collaborations], Phys. Rev. Lett. **120**, 042001 (2018).
- [2] W. Bernreuther and Z.-G. Si, Nucl. Phys. B **837** (2010) 90.
- [3] W. Bernreuther, M. Fuecker, and Z.-G. Si, Phys. Rev. D **74** 113005 (2006).
- [4] S. Moretti, M. Nolten, and D. Ross, Phys.Lett. B**639** (2006) 513.
- [5] D. Krohn, T. Liu, J. Shelton, and L.-T. Wang, Phys. Rev. D **84** 074034 (2011).
- [6] S. Fajfer, J. F. Kamenik, and B. Melic, J. High Energy Phys. **08** (2012) 114.
- [7] A. Brandenburg, Z.-G. Si, and P. Uwer, Phys. Lett. B **539** (2002) 235.

CDF Run II Prelim (9.1 fb <sup>-1</sup> )		$t\bar{t} \rightarrow l^+l^- + 2jets + \cancel{E}_T$		
Sources	Helicity		Transverse	
	CPC	CPV	CPC	CPV
	(-0.130)	(-0.046)	(-0.077)	(-0.111)
PDF	+0.015 -0.016	+0.002 -0.004	+0.006 -0.003	+0.002 -0.008
ISR/FSR	±0.018	±0.015	±0.030	±0.012
JES	±0.045	±0.003	±0.005	±0.005
Renormalization Scale	±0.013	±0.007	±0.020	±0.031
Top Quark Mass	±0.050	±0.006	±0.047	±0.014
MC Generator	±0.076	±0.014	±0.049	±0.016
Color Reconnection	±0.009	±0.013	±0.011	±0.022
Parton Showering	±0.014	±0.012	±0.045	±0.012
Background Shape	+0.029 -0.028	±0.028	+0.039 -0.040	±0.028
Total Syst.	±0.111	±0.040	±0.098	+0.055 -0.056
Stat.	+0.114 -0.109	±0.123	±0.177	+0.146 -0.145
Total Uncertainty	+0.159 -0.155	±0.129	±0.203	±0.156

Table 6: Systematic uncertainties in  $\alpha P$  for CPC and CPV cases in helicity and transverse bases. The uncertainties are evaluated at the resulting  $\alpha P$  value shown in the parentheses. The background shape uncertainty is obtained by quadratically subtracting the statistical only uncertainty from the uncertainty obtained from the likelihood maximization.

- [8] T. Aaltonen *et al.* [CDF Collaboration], Phys. Rev. D **88**, 091103 (2013).
- [9] T. A. Aaltonen *et al.* [CDF Collaboration], Phys. Rev. D **93**, 112005 (2016).
- [10] S. Alioli, S.-O. Moch, and P. Uwer, J. High Energy Phys. 01 (2012) 137; P. Nason, J. High Energy Phys. 11 (2004) 040; S. Frixione, P. Nason, and C. Oleari, J. High Energy Phys. 11 (2007) 070; S. Alioli, P. Nason, C. Oleari, and E. Re, J. High Energy Phys. 06 (2010) 043.
- [11] T. Sjöstrand, S. Mrenna, and P. Z. Skands, J. High Energy Phys. 05 (2006) 026.
- [12] E. Gerchtein and M. Paulini, eConf **C0303241**, TUMT005 (2003).
- [13] M. Baumgart and B. Tweedie, J. High Energy Phys. **08** (2013) 072.
- [14] W. Bernreuther, A. Brandenburg, and P. Uwer, Phys. Lett. B **368** (1996) 153.
- [15] W. Bernreuther, D. Heisler, and Z.-G. Si, J. High Energ. Phys. 12 (2015) 026.
- [16] G. L. Fogli, E. Lisi, A. Marrone, D. Montanino, and A. Palazzo, Phys. Rev. D **66** 053010 (2002).

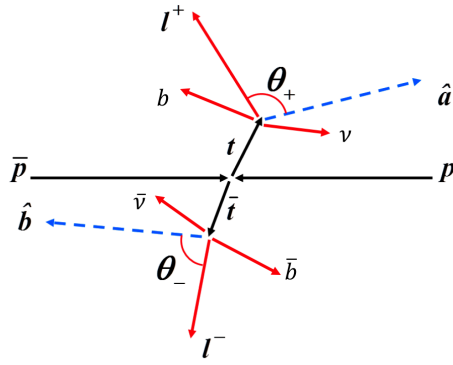


Figure 1: The opening angle  $\theta_+$  ( $\theta_-$ ) between positively (negatively) charged lepton  $l^+$  ( $l^-$ ) momentum direction and the quantization axis  $\hat{a}$  ( $\hat{b}$ ) in the top (antitop) rest frame.

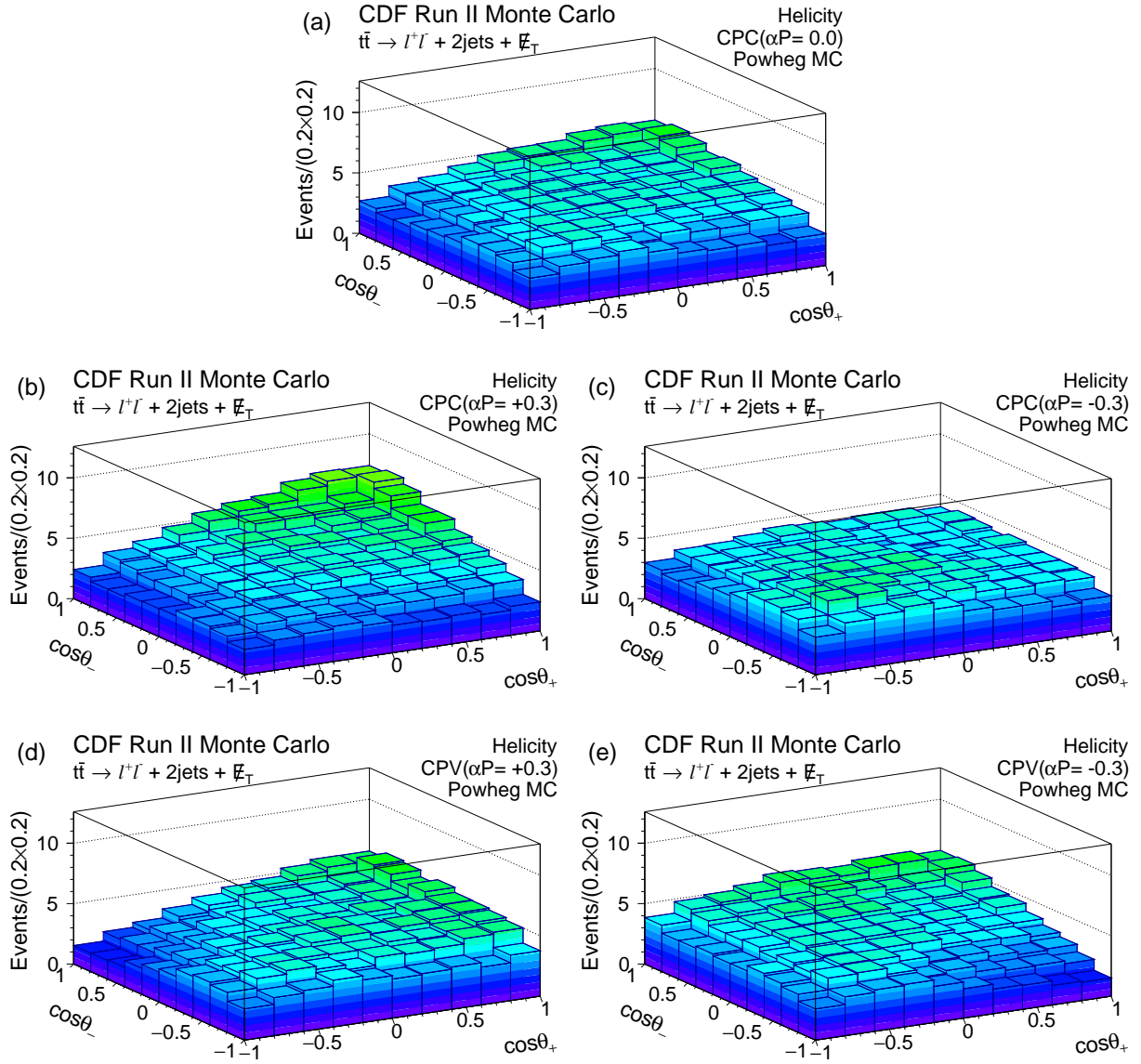


Figure 2: The signal  $(\cos\theta_+, \cos\theta_-)$  templates for the helicity basis of (a) CPC and CPV at  $\alpha P = 0$  (b) CPC at 0.3, (c) CPC at -0.3, (d) CPV at 0.3, and (e) CPV at -0.3.

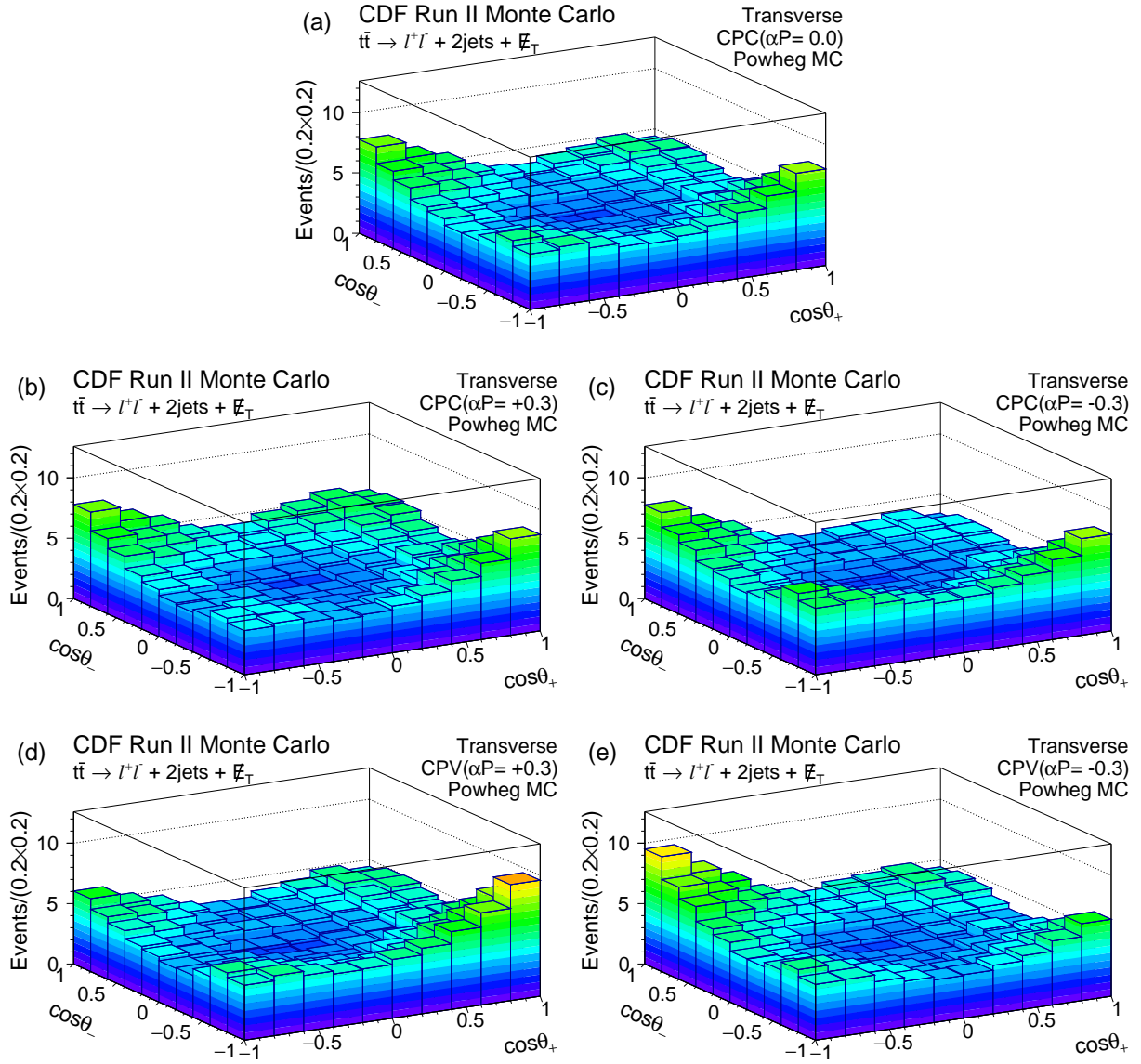


Figure 3: The signal  $(\cos\theta_+, \cos\theta_-)$  templates for the transverse basis of (a) CPC and CPV at  $\alpha P = 0$  (b) CPC at 0.3, (c) CPC at -0.3, (d) CPV at 0.3, and (e) CPV at -0.3.

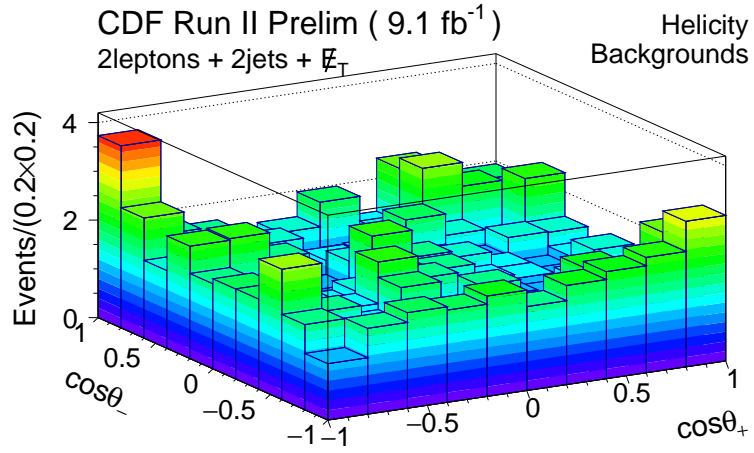


Figure 4:  $(\cos \theta_+, \cos \theta_-)$  distribution of two leptons for total background in helicity basis.

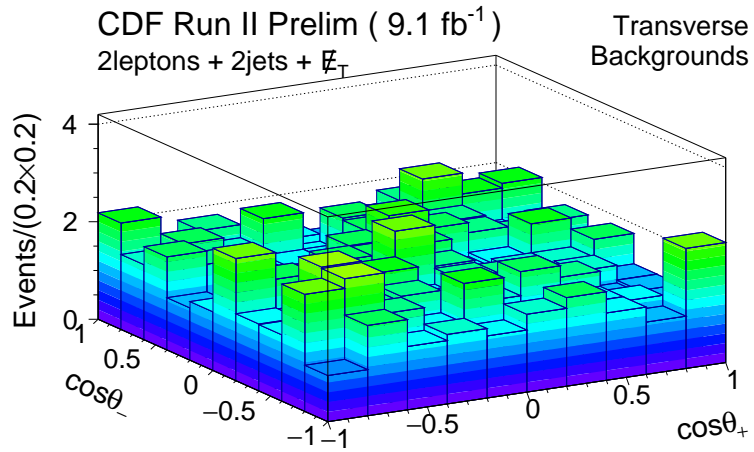


Figure 5:  $(\cos \theta_+, \cos \theta_-)$  distribution of two leptons for total background in transverse basis.





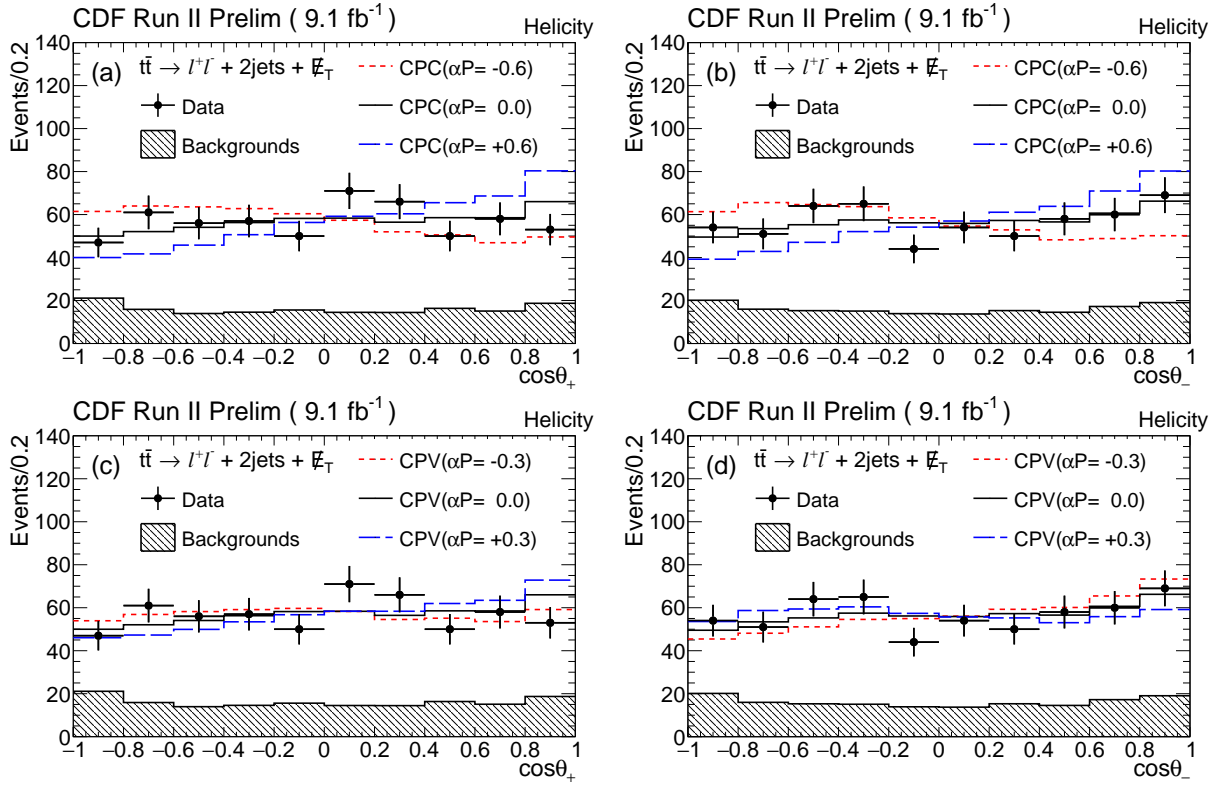


Figure 8: (a)  $\cos\theta_+$  and (b)  $\cos\theta_-$  distributions of CPC helicity and (c)  $\cos\theta_+$  and (d)  $\cos\theta_-$  of CPV helicity. Data is compared with the signal+background templates of  $\alpha P = -0.6$  ( $-0.3$ ) (red dashed),  $\alpha P = 0$  (black dotted), and  $\alpha P = 0.6$  ( $0.3$ ) (blue dashed) for CPC (CPV).

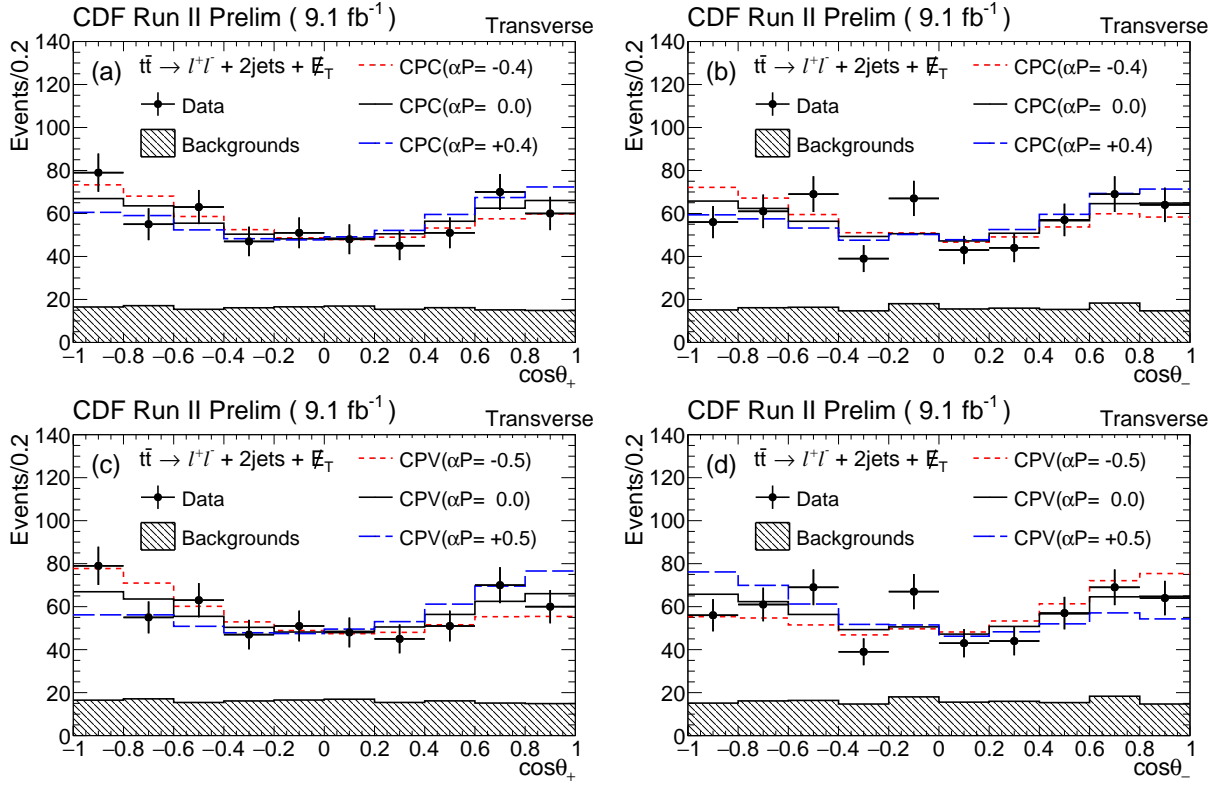


Figure 9: (a)  $\cos\theta_+$  and (b)  $\cos\theta_-$  distributions of CPC transverse and (c)  $\cos\theta_+$  and (d)  $\cos\theta_-$  distributions of CPV transverse. Data is compared with signal+background templates of  $\alpha P = -0.4(-0.5)$  (red dashed),  $\alpha P = 0$  (black dotted), and  $\alpha P = 0.4(0.5)$  (blue dashed) for CPC (CPV).

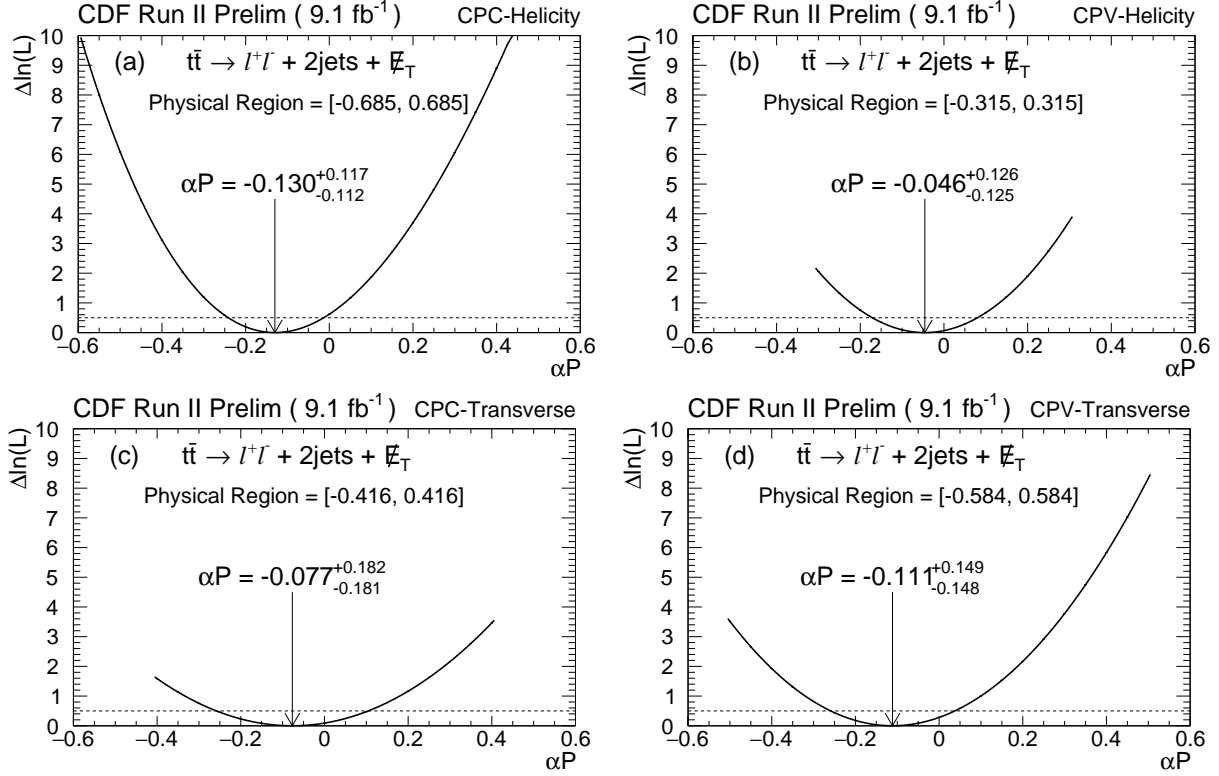


Figure 10: Likelihood difference distributions of the fit of (a) CPC helicity, (b) CPV helicity, (c) CPC transverse, and (d) CPV transverse. The dashed line shows the  $1\sigma$  difference. The likelihood fitting is performed in the physical region (Table 3).

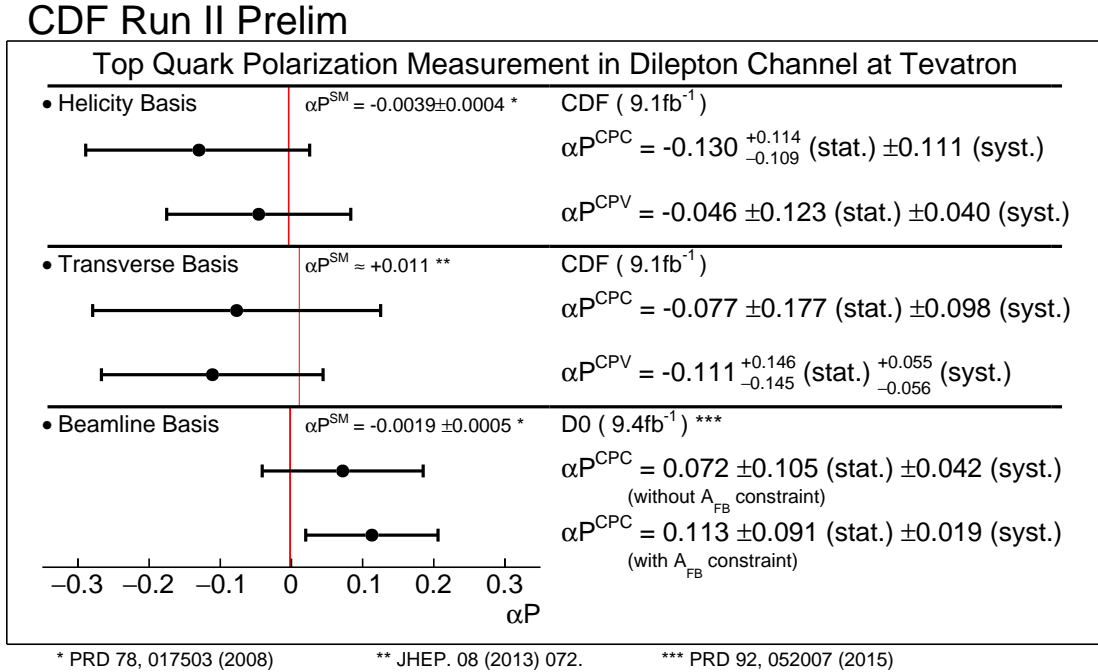


Figure 11: Summary of measurements of top quark polarization in the dilepton channel at Tevatron.